Tetrahedron Letters 55 (2014) 6131–6136

Contents lists available at ScienceDirect

Tetrahedron Letters

journal homepage: www.elsevier.com/locate/tetlet

1,8-Naphthalimide-based colorimetric and fluorescent sensor for recognition of GMP, TMP, and UMP and its application in in vivo imaging

Li Mei Zhang [a], Lin E. Guo [a], Xue Mei Li [c], Yong Gang Shi [b], Gao Fen Wu [b], Xiao Guang Xie [a], Ying Zhou [a,*], Qi Hua Zhao [a,*], Jun Feng Zhang [b,*]

[a] College of Chemical Science and Technology, Yunnan University, Kunming 650091, China
[b] College of Chemistry and Chemical Engineering, Yunnan Normal University, Kunming 650500, China
[c] Department of Safety Evaluation, Technology Center of China Tobacco Yunnan Industrial Co., Ltd, Kunming 650231, China

ARTICLE INFO

Article history:
Received 21 July 2014
Revised 11 September 2014
Accepted 15 September 2014
Available online 18 September 2014

Keywords:
Sensor
Colorimetric and fluorescent
Nucleotide
Naphthalimide
In vivo imaging

ABSTRACT

In this study, a series of 1,8-naphthalimide-based analogs were developed for fluorescence imaging of nucleotides in *Caenorhabditis elegans*. In DMSO, compound **1** proved to be an effective and selective colorimetric and fluorescent sensor for recognition of GMP, TMP, and UMP over other structurally similar nucleotides. Among all the tested nucleotides, only the addition of GMP, TMP, and UMP resulted in a fluorescence color change from blue to brown with a fluorescence enhancement of more than 600-fold, with the colorless solution turning brown. NMR spectroscopic titration, theoretical calculations, and spectral tests performed using various solvent compositions confirmed that compound **1** formed multiple hydrogen bonds with the related base groups in the nucleotide. Compound **1** demonstrated its utility as a fluorescent chemosensor for detecting GMP, TMP, and UMP in in vivo imaging of GMP, TMP, and UMP in *C. elegans*.

Introduction

In recent years, development of sensing systems and methods to recognize biologically and environmentally important species has emerged as a significant research area in the field of chemical sensors.[1] Nucleotides are active targets of fluorescence recognition,[2] and they have attracted remarkable attention due to their biological significance. Compared to the well-investigated adenosine-triphosphate (ATP), sensing systems to recognize other nucleotides and nucleotides have rarely been studied. Importantly, other nucleoside polyphosphates also play pivotal roles in various physiological events. For example, adenosine monophosphate (AMP) plays significant roles in bioenergetics, metabolism, and transfer of genetic information; and guanosine monophosphate (GMP) acts as an intermediate in the synthesis of nucleic acids and plays an important role in several metabolic processes.[3] Thymidine nucleotides, including thymidine-monophosphate (TMP), -diphosphate (TDP) and -triphosphate (TTP), synthesized in vivo from thymidine, are essential building blocks in DNA replication and cell division.[4] However, due to the similarities in the structures of the nucleotides, the design and synthesis of a chemosensor for the recognition of a certain nucleotide among various structurally similar nucleoside polyphosphates remain a fundamental challenge.[5]

Recently, we reported a series of 1,8-naphthalimide-based derivatives displaying selective colorimetric and fluorescence changes toward the target molecules.[6] Therefore, the objective of this study was to design an efficient nucleotide-selective colorimetric and fluorescent sensor, based on 1,8-naphthalimide, to explore its biological application in in vivo imaging of *Caenorhabditis elegans*.

In this study, three 1,8-naphthalimide-based analogs were synthesized. Compound **1**, a nucleotide-selective fluorescent sensor, can sense the binding process of GMP, TMP, and UMP by distinct colorimetric and fluorescent changes. The results of fluorescence tests revealed that compared to the other examined nucleotides, only GMP, TMP, and UMP generated a significant fluorescence response with compound **1**, with a fluorescence enhancement of more than 600-fold. Multiple hydrogen bonds, formed between the amide NH group of compound **1** and related base groups in the nucleotides, as well as deprotonation of NH explained the unique response of compound **1** in nucleotide sensing among the three synthesized analogs. In in vivo imaging tests of *C. elegans*,

* Corresponding authors.
E-mail addresses: yingzhou@yun.edu.cn (Y. Zhou), qhzhao@yun.edu.cn (Q.H. Zhao), junfengzhang@aliyun.com (J.F. Zhang).

http://dx.doi.org/10.1016/j.tetlet.2014.09.074
0040-4039/

an obvious blue to brown fluorescence change was clearly observed; demonstrating that compound **1** exhibited excellent cell permeability and it could combine with GMP, TMP, and UMP in different organs to trace their enrichment and distribution.

Results and discussion

In the design of the three 1,8-naphthalimide-based analogs (Scheme 1), we introduced O and N, as hydrogen bond acceptors, in the 4 position of 1,8-naphthalimide, in an attempt to promote hydrogen bond interactions with nucleotides. An acryloyl group and a (*e*)-2-butenoyl group were introduced in compounds **1**–**3** to compare the steric hindrances. Compounds **5**–**8** were synthesized with improved yields using a previously reported procedure.[7] Compounds **1**–**3** were synthesized in high yields, and the target compounds were purified prior to characterization. Detailed experimental procedures and ^{1}H and ^{13}C NMR spectra are explained in the Supporting information. The spectroscopic data of compounds **1**–**3** are listed in Table S1. In DMSO, compounds **1**–**3** displayed emission bands mainly in the regions of 415–463 nm, with weak fluorescent intensities. The results showed that the characteristic of the substituent did not significantly influence the luminescence of compounds **1**–**3**.

To clearly investigate the interaction of compounds **1**–**3** with nucleotide, the ultraviolet–visible (UV–Vis) absorption and fluorescence spectra of **1**–**3** were first studied in DMSO. ATP, ADP, AMP, GTP, GDP, GMP, UTP, UDP, UMP, and TMP were used to measure the selectivity of probes **1**–**3**. Spectra for all the nucleotides were recorded after 3 min of the addition of 10 equiv of each of the above mentioned molecules. Figure 1a shows that in the absence of nucleotide, compound **1** exhibits a major absorption band centered at 375 nm in DMSO. Only the addition of GMP, UMP, and TMP led to obvious red shifts from 375 to 500 nm in the absorption maximum. These red shifts resulted in dramatic color changes in the solution (colorless to brown). No significant spectrum change was observed in the presence of other nucleotides. Addition of different nucleotides to the solution of compounds **2**–**3** results in a similar obvious increase in the absorption maximum at 480 nm for ADP, GTP, GMP, UMP, and TMP, with the color of the solution changing from colorless to yellow as shown in Figures S1 and S2. Moreover, a slight decrease in the intensity of the peaks around 330 nm was observed for compounds **2**–**3** revealing that the selectivity of compounds **2**–**3** in absorption toward the tested nucleotides was not as good as that of **1**.

Compared to other examined nucleotides, only UMP, TMP, and GMP, when added to compound **1**, generated a significant

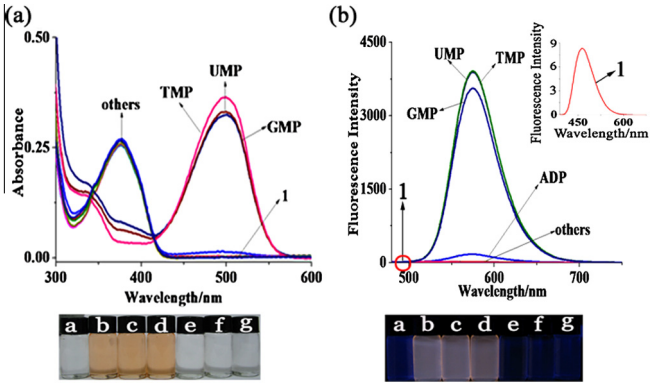

Figure 1. (a) Absorbance spectra of **1** (2.0×10^{-5} M) in DMSO with 10 equiv of ATP, ADP, AMP, GTP, GDP, GMP, UTP, UDP, UMP and TMP, down: the picture of **1** and **1** upon the addition of 10 equiv of selected ions (a: **1**, b: GMP, c: UMP, d: TMP, e: ATP, f: UTP, g: UDP); (b) fluorescence spectra of **1** (2.0×10^{-5} M) in DMSO with 10 equiv of ATP, ADP, AMP, GTP, GDP, GMP, UTP, UDP, UMP and TMP, down: the fluorescence picture of **1** and **1** upon the addition of 10 equiv of selected ions (a: **1**, b: GMP, c: UMP, d: TMP, e: ATP, f: UTP, g: UDP). Inset: the fluorescence spectrum of **1**.

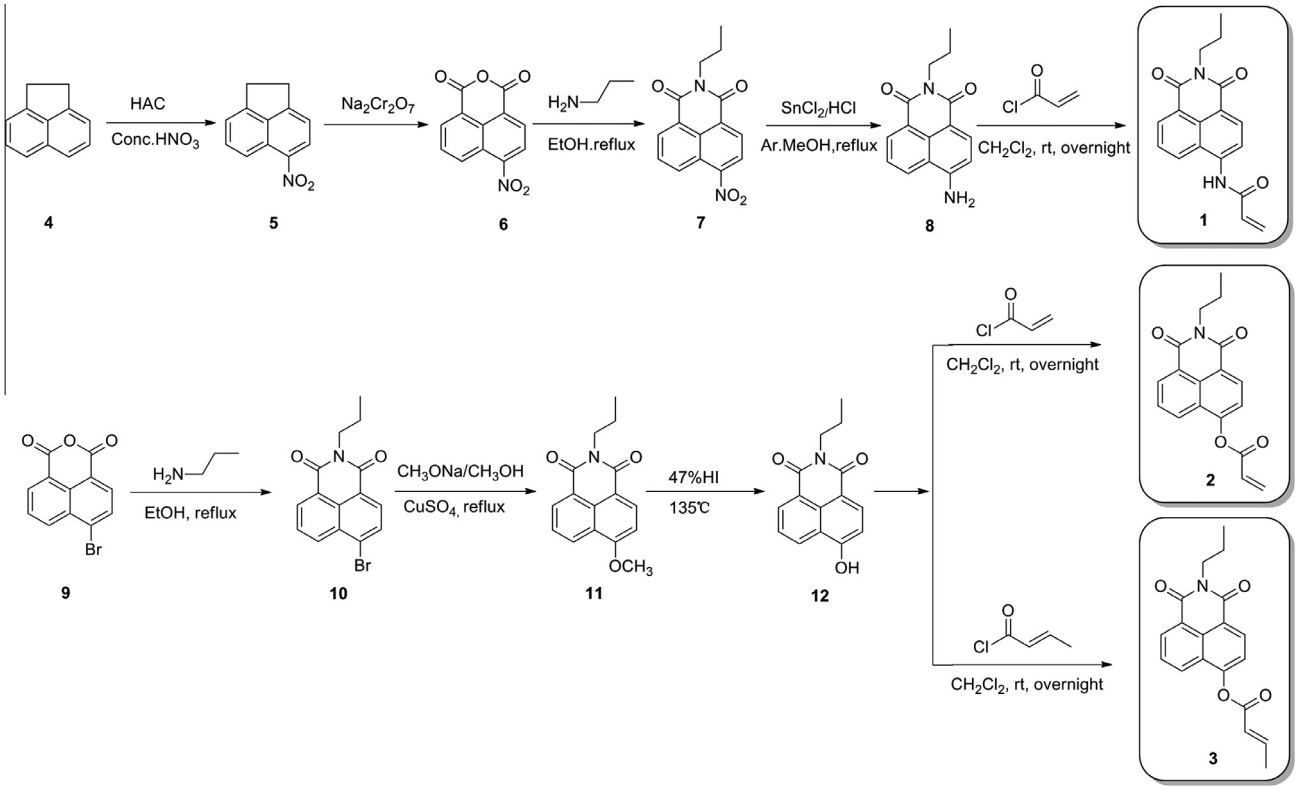

Scheme 1. The synthetic route of compounds **1**–**3**.

'turn-on' fluorescence response of the peak at 572 nm with 109 nm red-shift corresponding to a fluorescent change in color from blue to orange (Fig. 1b). A significant fluorescence enhancement of up to 690-fold for GMP, 635-fold for UMP and 690-fold for TMP was observed indicating high selectivity of **1** for UMP, GMP, and TMP compared to the other tested nucleotides. Addition of nucleotides to solutions of compounds **2**–**3** in DMSO did not result in a regular change in the fluorescence spectra (Figs. S1 and S2) revealing that **1** exhibits the best fluorescent selectivity toward the tested nucleotides, such as GMP, UMP, and TMP, among the three synthesized analogs. Therefore, further investigations and tests were performed on **1**.

To obtain insight into the binding of nucleotides with **1**, the UV–Vis and fluorescence spectra of **1** upon titration with different equivalents of GMP (Fig. 2), UMP (Fig. S3) and TMP (Fig. 3) are recorded. Figure 2a shows that upon titration with GMP, the absorbance band at 500 nm increased sharply; however, the peak at 375 nm decreased slowly. Addition of GMP to a solution of **1** led to an increase in the fluorescence emission intensity at 575 nm by 690-fold which reached a maximum value after 10 equiv of GMP was added. The solutions of **1** treated with GMP undergo drastic changes in their fluorescence spectroscopic properties corresponding to a change in color from blue to orange as shown in Figure 2b. A similar change in UV–Vis spectra with a sharp decrease in the intensity at 375 nm and an increase at 500 nm was observed for TMP. Moreover, the fluorescence intensity of the peak at 575 nm, attributed to the interaction of **1** with TMP, is enhanced significantly by 690-fold and levels up on the addition of 5 equiv of TMP as shown in Figure 3b. Figure S3 demonstrates that the addition of UMP to a solution of **1** leads to a decrease in the intensity of absorbance at 375 nm and an increase in the band at 498 nm. 635-fold increase in fluorescence was observed at 575 nm with the addition of 5 equiv of UMP.

The binding constant for a 1:1 receptor–nucleotide complex formation was determined for **1** and UMP, TMP, and GMP by using the Job-plot equations (Figs. S5–S7). The corresponding binding constants of **1** with nucleotides were estimated to be 2.09×10^3, 2.77×10^4, and $2.31 \times 10^4\ M^{-1}$ for GMP, UMP, and TMP, respectively (Figs. S11–S13). Stabilities of the complexes of nucleotides with **1** were found to be in the following order: **1**-TMP > **1**-UMP > **1**-GMP. The fluorescence intensity of **1** was linearly proportional to the concentrations (0–10 μM) of GMP, UMP, and TMP and detection limits as low as 1.48×10^{-7} M concentration of GMP, 1.45×10^{-6} M of UMP and 1.20×10^{-6} M of TMP were established using **1**, with a signal-to-noise ratio of 3 (Figs. S8–S10).

Figure 4 shows the UV–Vis absorption changes and fluorescence changes of **1**-GMP (1:10 equiv) using various solvent compositions. Upon increasing the water content while maintaining the concentration constant, the absorption of **1**-GMP at 490 nm dropped in intensity with a concomitant growth of a new band at 372 nm with well-defined isosbestic points at 340 and 415 nm. Moreover, the intense emission at 575 nm decreased with the increasing water compositions. Drastic reverse color changes from brown to colorless displayed by solutions of **1**-GMP were due to the interference from the water molecules. Similar spectral changes are observed for **1**-TMP (Fig. 5) and **1**-UMP (Fig. S3) with a successive increase in the water content indicating that **1**-nucleotides complexes (**1**-GMP, **1**-TMP and **1**-UMP) are affected significantly by change in the polarity of the solvent and sensitive to the microenvironment.

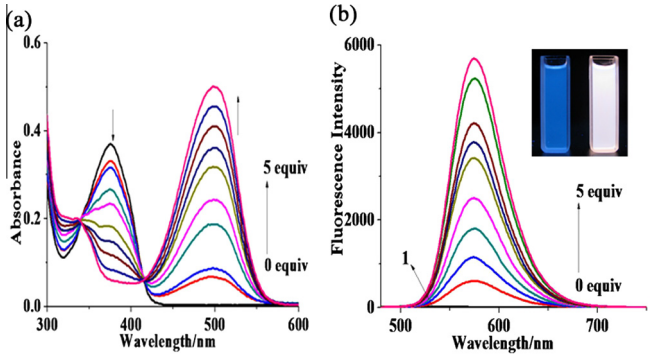

Figure 3. (a) Absorbance titration spectra of **1** (2.0×10^{-5} M) in the presence of varying concentrations of TMP in DMSO. (b) Fluorescence emission titration spectra of **1** (2.0×10^{-5} M) in the presence of varying concentrations of TMP in DMSO.

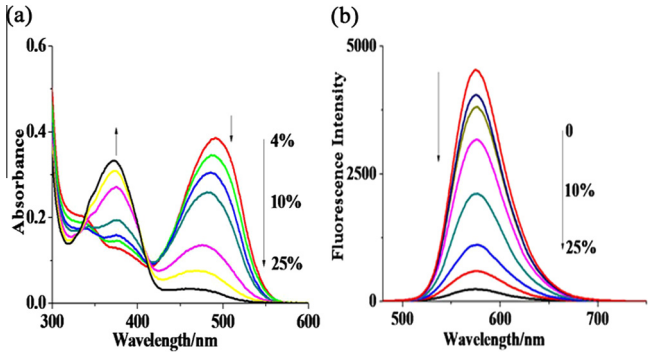

Figure 4. (a) Absorbance spectra of **1** (2.0×10^{-5} M) in DMSO with 10 equiv of GMP containing water (4%, 6%, 8%, 10%, 15%, 20%, 25%, v/v). (b) Fluorescence spectra of **1** in DMSO with 10 equiv of GMP containing water (0%, 2%, 6%, 8%, 10%, 15%, 20%, 25%, v/v).

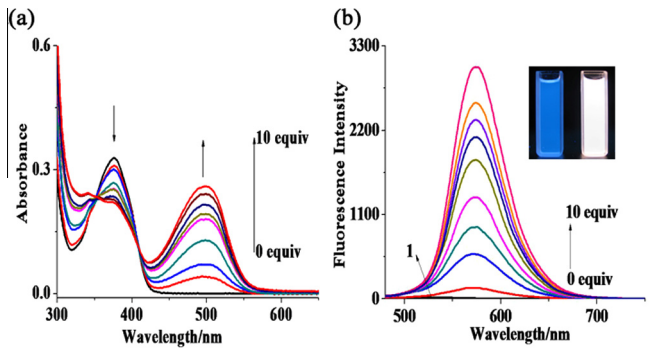

Figure 2. (a) Absorbance titration spectra of **1** (2.0×10^{-5} M) in the presence of varying concentrations of GMP in DMSO. (b) Fluorescence emission titration spectra of **1** (2.0×10^{-5} M) in the presence of varying concentrations of GMP in DMSO.

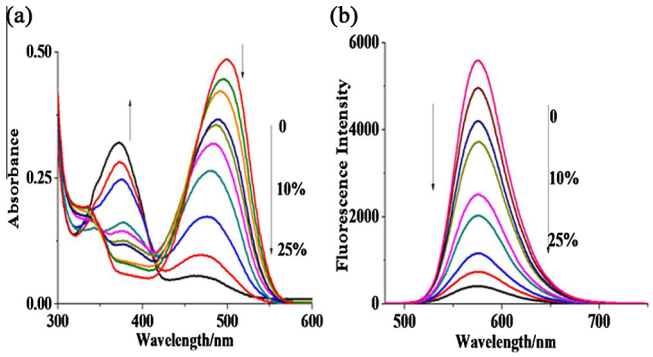

Figure 5. (a) Absorbance spectra of **1** (2.0×10^{-5} M) in DMSO with 10 equiv of TMP containing water (0%, 2%, 4%, 6%, 8%, 10%, 12%, 15%, 20%, 25%, v/v). (b) Fluorescence spectra of **1** in DMSO with 10 equiv of TMP containing water (0%, 2%, 4%, 8%, 10%, 12%, 15%, 20%, 25%, v/v).

Further, theoretical calculations were performed to confirm the binding patterns of **1** with GMP, UMP, and TMP. In this study, the density functional theory (B3LYP/6-31G* level)[8] was used to describe the binding pattern and H-bond interactions. The results showed that multi-hydrogen bonds were first formed between the amide NH group of **1** and related base groups in the nucleotides. As reported in the literatures,[9] the large red-shift of the UV–Vis absorption and fluorescence spectra of **1** could be attributed to the deprotonation of N–H, thus, explaining the unique response of **1** among the three synthesized analogs. Amide NH group is a principal H-bond donor, and the similar structural features of uracil group (in UMP), thymine group (in TMP), and guanine group (in GMP) are the major reasons for the multi-hydrogen bond formation (Fig. 6a), in this study on nucleotide recognition. Figure 6b exhibits that each molecule of **1** is connected to one molecule of UMP, TMP, and GMP via two O···H—N bonds. Distances of O···H bonds are 1.831 and 1.808 Å in **1**-UMP, 1.839 and 1.805 Å in **1**-TMP, and 1.837 and 1.732 Å in **1**-GMP. All the distances of O···H—N in these three cases are in good agreement with the description of intermolecular hydrogen bonds, strongly supporting the H-bond interactions in the recognition process. Compared to the above mentioned three nucleotides, adenine group in AMP (Fig. 6a) could not form multi-hydrogen bonds with **1**; therefore, no obvious signal response was observed for AMP. Meanwhile, the intramolecular H-bond formation of UDP was calculated. It showed that two intramolecular hydrogen bonds are formed inside one UDP molecule, which explained why no response toward UDP was found (Fig. S30).

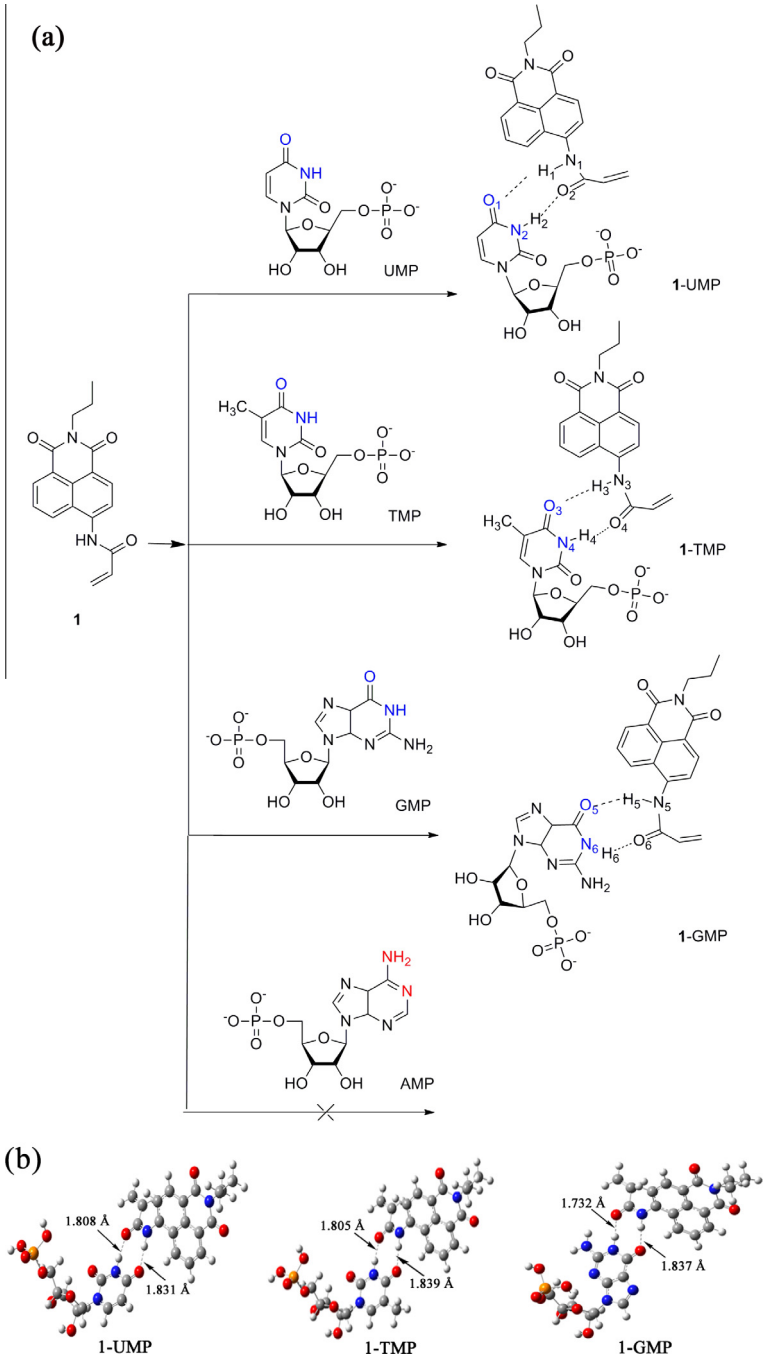

Figure 6. (a) The proposed binding mechanism of compound **1** with UMP, TMP and GMP. (b) Calculated structure of **1** binding with UMP, TMP and GMP.

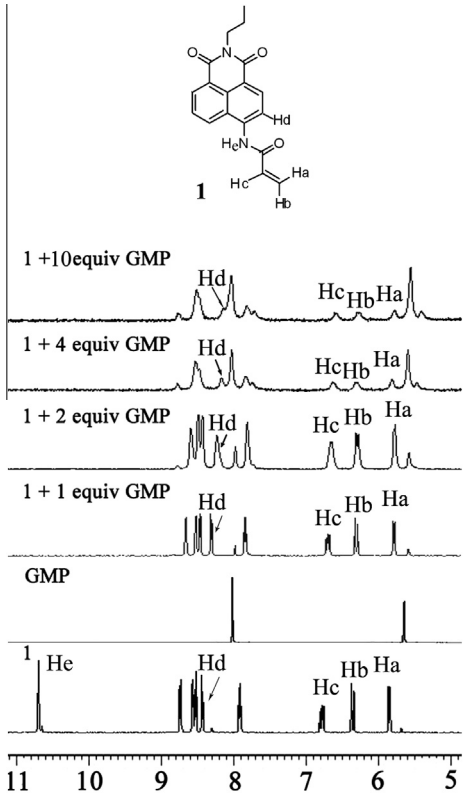

Figure 7. The ^{1}H NMR spectra of compound **1** (0.012 mM) with GMP in DMSO-d_6; equivalents of GMP are related to the concentration of compound **1**.

Further evidence for the binding interactions of **1**-GMP (Fig. 7), **1**-TMP (Fig. S14) and **1**-UMP (Fig. S15) was obtained by NMR titration studies. Figure 7 demonstrates that, with the addition of varying concentrations of GMP to **1** (0.012 mM) in DMSO-d_6, the upfield shifts of protons (Ha, Hb, Hc, and Hd) are observed indicating the occurrence of hydrogen bond interactions between **1** and GMP in the **1**-GMP complex. The disappearance of He is the evidence for the deprotonation of N–H. Results of NMR spectroscopic analysis significantly supported the sensing mode of **1** and the related nucleotide.

To demonstrate the feasibility of **1** for its application in in vivo imaging, fluorescence imaging tests were performed in *C. elegans*.[10] Previously, the author successfully used *C. elegans* to test and evaluate the toxicity levels of heavy metal mercury.[11] In the present study, the application of **1** in in vivo imaging was evaluated by visualizing the distribution of GMP, TMP, and UMP in nematodes incubated with nucleotide (100 μM) for 15 h. *C. elegans* larvae at developmental stage 4 (L4) were used. For demonstrating the fluorescence-imaging of accumulations of UMP, TMP, and GMP in the nematode, the previously exposed worms were incubated in centrifuge tube filled with 1 mL of M_9 buffer, containing 10 μM of **1**, at 20 °C for 1 h. Figure 8 shows that the addition of GMP, TMP, and UMP leads to a significant change in the color of the fluorescence from blue to yellowish-brown, demonstrating that **1** was readily internalized into *C. elegans* and it could trace the enrichment and distribution of the related nucleotide. The above mentioned results revealed that **1** exhibited excellent cell permeability and that it could be effectively utilized to monitor GMP, TMP, and UMP in living cells and *C. elegans*.

Conclusion

Of the three 1,8-naphthalimide-based analogs that were developed, compound **1** has demonstrated effective and selective colorimetric and fluorescent sensing for recognition of GMP, TMP and UMP over other structurally similar nucleotides. Among all the tested nucleotides, addition of only GMP, TMP, and UMP resulted in significant fluorescence enhancements, and the colorless solution turned brown. Compound **1**'s nucleotide binding mechanism involves multiple hydrogen bonds with the related base groups in the nucleotide and the deprotonation of the nitrogen acceptor at position 4 being the primary reasons for successful recognition. This binding mechanism was supported by NMR spectroscopic titration, theoretical calculations and spectral tests performed using various solvent compositions. Compound **1** was successfully applied to fluorescence imaging for GMP, TMP and UMP in *C. elegans*, demonstrating its utility as a fluorescent chemosensor for detecting GMP, TMP, and UMP in in vivo imaging.

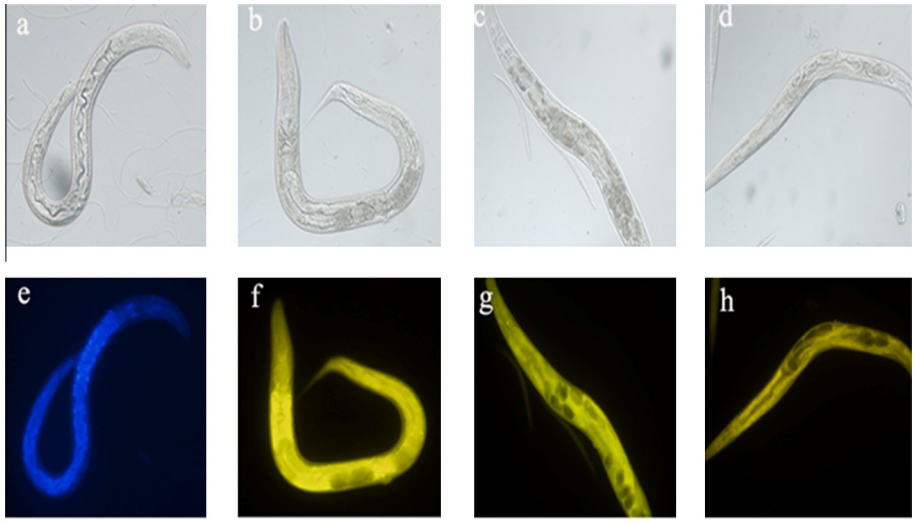

Figure 8. Phase contrast (top) and fluorescence images (bottom) of *C. elegans*. *C. elegans* were exposed to 100 μM GMP, UMP, and TMP for 15 h and then treated with 10 μM of **1** for 1 h. (e) Fluorescence images of *C. elegans* treated with 10 μM of **1** only. (f) Fluorescence images of *C. elegans* treated with 100 μM GMP for 15 h and 10 μM of **1** for 1 h. (g) Fluorescence images of *C. elegans* treated with 100 μM UMP for 15 h and 10 μM of **1** for 1 h. (h) Fluorescence images of *C. elegans* treated with 100 μM TMP for 15 h and 10 μM of **1** for 1 h.

Acknowledgments

This work was supported by the Natural Science Foundation of China (NSFC Grant Nos. 21102127, 21262045, 21262050, 21302165, 21371151 and 21462050); the Foundation of the Department of Science and Technology of the Yunnan Province of China (Nos. 2011FB013, 2011FB047 and 2013HB062); and Student Research Training of the Yunnan Normal University (KY-2013-125).

Supplementary data

Supplementary data associated with this article can be found, in the online version, at http://dx.doi.org/10.1016/j.tetlet.2014.09.074.

References and notes

1. (a) Chen, X. Q.; Zhou, Y.; Peng, X. J.; Yoon, J. *Chem. Soc. Rev.* **2010**, *39*, 2120–2135; (b) Wade, C. R.; Broomsgrove, A. E. J.; Aldridge, S.; Gabbaï, F. P. *Chem. Rev.* **2010**, *110*, 3958–3984; (c) Zhang, J. F.; Zhou, Y.; Yoon, J.; Kim, J. S. *Chem. Soc. Rev.* **2011**, *40*, 3416–3429; (d) Ying, Z.; Yoon, J. *Chem. Soc. Rev.* **2012**, *41*, 52–67; (e) Wenzel, M.; Hiscock, J. R.; Gale, P. A. *Chem. Soc. Rev.* **2012**, *41*, 480–520; (f) Yuan, L.; Lin, W. Y.; Zhang, K. B.; Huang, W. M. *Chem. Soc. Rev.* **2013**, *42*, 622–661.
2. (a) Zhou, Y.; Xu, Z. C.; Yoon, J. *Chem. Soc. Rev* **2011**, *40*, 2222–2235; (b) Kellenberger, C. A.; Wilson, S. C.; Lee, J. S.; Hammond, M. C. *J. Am. Chem. Soc.* **2013**, *135*, 4906–4909; (c) Cisar, E. A. G.; Nguyen, N.; Rosen, H. *J. Am. Chem. Soc.* **2013**, *135*, 4676–4679; (d) Noé, M. S.; Sinkeldam, R. W.; Tor, Y. *J. Org. Chem.* **2013**, *78*, 8123–8128; (e) Ema, T.; Okuda, K.; Watanabe, S.; Yamasaki, T.; Minami, T.; Esipenko, A.; Anzenbacher, P. *Org. Lett.* **2014**, *16*, 1302–1305; (f) Kong, J. C.; He, C.; Zhang, X. L.; Meng, Q. T.; Duan, C. Y. *Dyes Pigments* **2014**, *101*, 254–260; (g) Banerjee, S.; Kitchen, J. A.; Gunnlangsson, T.; Kelly, J. M. *Org. Biomol. Chem.* **2012**, *10*, 3033–3043; (h) Banerjee, S.; Kitchen, J. A.; Gunnlaugsson, T.; Kelly, J. M. *Org. Biomol. Chem.* **2013**, *11*, 5642–5655; (i) Kawai, K.; Kawabata, K.; Tojo, S.; Majima, T. *Bioorg. Med. Chem. Lett.* **2002**, *12*, 2363–2366; (j) Li, H. T.; Jiang, Z. Q.; Zhang, J.; Wang, X.; Pen, Y.; Wang, F.; Yu, S. Q. *Res. Chem. Intermed.* **2006**, *32*, 43–57.
3. (a) Molz, S.; Tharine, D.-C.; Decker, H.; Tasca, C. I. *Brain Res.* **2008**, *1231*, 113–120; (b) Nair, A. K.; Neelakandan, P. P.; Ramaiah, D. *Chem. Commun.* **2009**, 6352–6354.
4. Pullarkat, S.; Stoehlmacher, J.; Ghaderi, V.; Xiong, Y. P.; Ingles, S. A.; Sherrod, A.; Warren, R.; Tsao-Wei, D.; Groshen, S.; Lenz, H. J. *Pharmacogenomics J.* **2001**, *1*, 65–70.
5. Zhang, M.; Ma, W. J.; He, C. T.; Jiang, L.; Lu, T. B. *Inorg. Chem.* **2013**, *52*, 4873–4879.
6. (a) Duan, Y. L.; Shi, Y. G.; Chen, J. H.; Wu, X. H.; Wang, G. K.; Zhou, Y.; Zhang, J. F. *Tetrahedron Lett.* **2012**, *53*, 6544–6547; (b) Shi, Y. G.; Yao, J. H.; Duan, Y. L.; Mi, Q. L.; Chen, J. H.; Xu, Q. Q.; Guo, G. Z.; Zhou, Y.; Zhang, J. F. *Bioorg. Med. Chem. Lett.* **2013**, *23*, 2538–2542; (c) Zhao, L. Y.; Mi, Q. L.; Wang, G. K.; Chen, J. H.; Zhang, J. F.; Zhao, Q. H.; Zhou, Y. *Tetrahedron Lett.* **2013**, *54*, 3353–3358; (d) Shi, Y. G.; Duan, Y. L.; Chen, J. H.; Wu, X. H.; Zhou, Y.; Zhang, J. F. *Bull. Korean Chem. Soc.* **2013**, *34*, 63–67; (e) Zhao, L. Y.; Wang, G. K.; Chen, J. H.; Zhang, L. M.; Liu, B.; Zhang, J. F.; Zhao, Q. H.; Zhou, Y. *J. Fluorine Chem.* **2014**, *158*, 53–59.
7. (a) Huang, X.; Huang, S.; Zhai, B.; Zhang, Y.; Xu, Y.; Wang, Q. *Tetrahedron Lett.* **2012**, *53*, 6414–6417; (b) Xuan, W.; Pan, R.; Cao, Y.; Liu, K.; Wang, W. *Chem. Commun.* **2012**, 10669–10671; (c) Quintana-Espinoza, P.; García-Luis, J.; Amesty, Á.; Martín-Rodríguez, P.; Lorenzo-Castrillejo, I.; Ravelo, A. G.; Fernández-Pérez, L.; Machín, F.; Estévez-Braun, A. *Bioorg. Med. Chem.* **2013**, *21*, 6484–6495.
8. Frisch, M. J. et al *Gaussian 09, Revision A. 02*; Gaussian: Walling, CT, 2009 (see full Ref. in Supporting information).
9. (a) Zhang, J. F.; Lim, S. C.; Bhuniya, S.; Cho, B. R.; Kim, J. S. *Org. Lett.* **2011**, *13*, 1190–1193; (b) Qu, Y.; Hua, Y. H.; Jiang, Y. H.; Tian, H. *J. Polym. Sci., Part A: Polym. Chem.* **2009**, *47*, 1544–1552.
10. (a) Contreras, E. Q.; Chao, M. J.; Zhu, H. G.; Puppala, H. L.; Escalera, G.; Zhong, W. W.; Colvin, V. L. *Environ. Sci. Technol.* **2013**, *47*, 1148–1154; (b) Goel, A.; Sharma, A.; Kathuria, M.; Bhattacharjee, A.; Verma, A.; Mishra, P. R.; Nazir, A.; Mitra, K. *Org. Lett.* **2014**, *16*, 756–759; (c) Stupp, G. S.; Reuss, S. H. V.; Izrayelit, Y.; Ajredini, R.; Schroeder, F. C.; Edison, A. S. *ACS Chem. Biol.* **2013**, *8*, 309–313; (d) Bender, A.; Woydziak, Z. R.; Fu, L.; Branden, M.; Zhou, Z.; Ackley, B. D.; Peterson, B. R. *ACS Chem. Biol.* **2013**, *8*, 636–642.
11. Wang, G. K.; Mi, Q. L.; Zhao, L. Y.; Hu, J. J.; Guo, L. E.; Zou, X. J.; Xie, X. G.; Zhang, J. F.; Zhao, Q. H.; Zhou, Y. *Chem. Asian J.* **2014**, *9*, 744–748.